Adhesion and collapse of extreme ultraviolet photoresists and the role of underlayers

Roberto Fallica,[a,*] **Steven Chen**,[a,b] **Danilo De Simone**,[a] **and Hyo Seon Suh**[a]
[a]IMEC, Leuven, Belgium
[b]Karlsruhe Institute of Technology, Karlsruhe, Germany

Abstract. Pattern collapse and photoresist scumming are major limiting factors to achieve a failure-free process window in extreme ultraviolet lithography. Previous works on this topic have empirically proven the importance of matching photoresist and underlayer surface energy, and the role played by developer liquid in wet development. In this work, we extend those concepts and formulate a figure of merit for the free energy at the exposed and unexposed photoresist-underlayer-developer interfaces. This figure of merit provides a tool to optimize the underlayer surface energy components that best match a given photoresist and developer process. The model is tested against experimental patterning of a chemically amplified resist at pitch 32 nm and pitch 80-nm line spaces, successfully predicting the likelihood of pattern collapse and photoresist scumming. Moreover, we write a quantitative expression for the peeling force acting on photoresist lines owing to unbalanced capillary forces and the threshold energy at which film delamination onsets. It is shown that adhesion and scumming are two manifestations of the same phenomenon at these interfaces. © *2022 Society of Photo-Optical Instrumentation Engineers (SPIE)*
[DOI: 10.1117/1.JMM.21.3.034601]

Keywords: surface energy; adhesion; collapse; extreme ultraviolet; interface; developer.

Paper 22026G received May 20, 2022; accepted for publication Jul. 11, 2022; published online Jul. 25, 2022.

1 Introduction

Optical lithography based on extreme ultraviolet (EUV) wavelength is being deployed for high-volume manufacturing while the scaling of semiconductor devices continues unrelented.[1] For logic devices, EUV lithography is expected to enable technology nodes N3/N2, where the most challenging layers require dense patterns of pitch <28 nm.[1] Moreover, the thickness of the photoresist and related underlayers used in lithography is expected to shrink as well, so as to maintain an acceptable aspect ratio of line arrays and prevent pattern collapse. As a result, not only the resolution of the optical system and resist material matter, but also interfacial chemistry between resist, underlayer, and developer become increasingly relevant. These observations have been highlighted in previous studies on surface energy at the boundary between the photoresist and the first underlayer of the EUV lithography stack. Polar and nonpolar forces have been shown to play a role in photoresist line profile after development,[2] photoresist scumming in the trenches,[3] pattern collapse,[4] or delamination.[5] The surface tension of the developer impacts adhesion of micro bubbles on the films,[6] and its chemistry affects photoresist scumming and delamination, as was reported in pioneering works on tetrabutylammonium hydroxide.[7–9] The rinse liquid has also been demonstrated to influence the collapse margin and line width roughness (LWR).[10] All this research draws our attention to improving EUV performance through in-depth understanding of the interfacial properties. Such an example is the finding that pattern collapse can be minimized, at least empirically, by matching both surface energy components of photoresist and underlayer.

In this paper, we aim to capitalize on these empirical observations and concepts of surface energy components to build on a predictive figure of merit that can explain interfacial forces in EUV lithography. It is first important to acknowledge that the photoresist-underlayer-developer

*Address all correspondence to Roberto Fallica, roberto.fallica@imec.be

1932-5150/2022/$28.00 © 2022 SPIE

system has three surface energy combinations. In addition to that, we consider how the adhesion of these interfaces is affected by EUV exposure: the surface energy of photoresist after exposure is usually very different from unexposed resist (due to solubility switching), as well as that of underlayer. Using this approach, we get information on the interface in the line region (unexposed) and space region (exposed) independently, depending on whether we want more adhesion to avoid collapse in the line region or less adhesion to avoid scumming in the trenches. Besides, one of the origins of external force that causes pattern collapse is the capillary force during development, or more precisely, during rinse and drying. Heading toward advanced technology nodes, we are facing higher capillary force due to the scaling of the geometrical dimensions. Here, we point our attention to those conditions that cause the capillary force to become unbalanced and explain it on the account of geometrical factors, e.g., space width roughness (SWR), resist height, and space width. The usage of low surface tension rinse liquids is preferred to deionized water in pitch 28-nm EUV lithography for pattern collapse mitigation reasons. However, our methodology can be extended to the case of any rinse liquid by dialing in the appropriate value in the capillary force equation. Finally, we frame the unbalanced capillary force as the main competitor to the adhesion forces in the three phases system. By recognizing that pattern collapse is not a binary phenomenon, but a probabilistic one, a more refined statistical description is proposed.

2 Experimental Details and Methodology

2.1 *Lines/Spaces Patterning by EUV Lithography*

The NXE3400B EUV scanner was used to pattern a chemically amplified photoresist (CAR), 35-nm thickness, in dense lines/spaces (LS) patterns of ratio 1:1 and pitch ranging from 80 to 32 nm. Different underlayers, spin-coated or dry deposited, on Si bulk wafers were used as substrate. After EUV exposure, development and rinse took place in an EUV clean cluster track using a conventional process [0.26N tetramethyl ammonium hydroxide (TMAH) developer, and undisclosed rinse chemistry]. Metrology of critical dimension (CD) and LWR/SWR was carried out by CD scanning electron microscopy (CDSEM) and top-down imaging of areas of $\sim 1\ \mu\mathrm{m}^2$.

2.2 *Surface Energy and Free Energy at Interfaces, and the Work of Adhesion*

The surface energy components (polar, γ^p and dispersive, γ^d) of photoresists and underlayers were measured by sessile drop contact angle using two liquids (water and diiodomethane) according to Kaelble's method[11] and Owens and Wendt.[12] The total surface tension of the developer was measured by the pendant drop method[13] and its polar and dispersive components were found to be matching with values from the literature.[7,14] The free energy, γ, of any open surface is typically nonzero because of the energetically unfavorable discontinuity with vacuum at the molecular level. By depositing a new material (liquid or solid) on top of an open surface, a new interface forms, which can be energetically convenient and reduce the total free energy of the system. In the case of a liquid (1) dropped on a solid surface (2) the two individual free energies of each phase are reduced by an amount equal to their work of adhesion (W_{a12}) owing to Coulombic interactions and dispersive interactions. The work of adhesion of the (12) interface represents the energy required to separate (1) from (2) and counteracts the tendency to form a new interface as described in pioneering work by Fowkes:[15] in practice, larger values of W_{a12} indicate good surface energy matching and therefore smaller interfacial energy. The total interface energy is, therefore

$$\gamma_{12} = \gamma_1 + \gamma_2 - W_{a12}. \tag{1}$$

Because total surface energy is typically the sum of several components that account for molecular effects, in this work we consider the total free energy contribution of two components,

i.e., the polar and dispersive forces, therefore writing $\gamma = \gamma^p + \gamma^d$. The work of adhesion W_{a12} can be expressed as the geometric mean of the two surfaces' components

$$W_{a12} = 2\left(\sqrt{\gamma_1^d \gamma_2^d} + \sqrt{\gamma_1^p \gamma_2^p}\right). \tag{2}$$

Several empirical models have been proposed to describe the interfacial forces between two surfaces; in this work and Eq. (2), we use geometric mean (as in Johnson et al.[16]) rather than harmonic mean (as proposed by Wu[17]). The latter approach yields a smaller total W_{a12} because it gives more weight to the weakest of the two surfaces in comparison to the former method. The harmonic mean is therefore typically used for low total surface energy and high polar component solids. The photoresists and underlayers used in our work have a total surface energy of about 40 mN/m or more and are more dispersive than polar; deionized water and developer have a surface tension of around 70 mN/m as reported previously.[17–20] For this reason, several experimental studies also adopted the geometric mean for the calculation of adhesion of solid/solid and polymer/polymers interfaces.[21–23]

Combining the previous expressions, we obtain that the interfacial energy can be expressed as a function of the difference between polar and dispersive components, respectively:

$$\gamma_{12} = \left(\sqrt{\gamma_1^d} - \sqrt{\gamma_2^d}\right)^2 + \left(\sqrt{\gamma_1^p} - \sqrt{\gamma_2^p}\right)^2. \tag{3}$$

Equation (3) indicates that the minimum free energy at an interface happens between two identically matching materials.

2.3 *W_3 Metric for Three-Interfaces Systems*

Let us now extend this concept to include the role of developer in forming new interfaces with photoresist and underlayer during development. Wet development is the workhorse process step in lithography processing for chemically amplified resists used in EUV and previous technologies (although dry development photoresist platforms are recently proposed for high volume manufacturing[24]). The introduction of developer forms a total of six interfaces with photoresist and underlayer, both exposed and unexposed to EUV light. For the unexposed areas, the energy balance can be written in the form of a figure of merit W_3 equal to the interfacial energy of the two newly formed interfaces (PR/DEV and UL/DEV) minus the original interface energy (PR/UL)

$$W_3 = (\gamma_{\mathrm{PR/DEV}} + \gamma_{\mathrm{UL/DEV}}) - \gamma_{\mathrm{PR/UL}}. \tag{4}$$

Essentially, Eq. (4) predicts whether the liquid developer shall be able to replace the existing photoresist/underlayer interface ($W_3 \leq 0$) or not ($W_3 \geq 0$). In the case of positive tone processing, it is desirable for the unexposed photoresist line to have W_3 as large as possible. Similarly, a new figure $W_{3\,\mathrm{exp}}$ can be defined for the interfaces present in exposed areas of photoresist (trenches)

$$W_{3\,\mathrm{exp}} = (\gamma_{\mathrm{PR\,exp/DEV}} + \gamma_{\mathrm{UL\,exp/DEV}}) - \gamma_{\mathrm{PR\,exp/UL.}} \tag{5}$$

In this latter case, the surface energy of exposed photoresist and exposed underlayers have to be used. To minimize photoresist residues and scumming in exposed areas, $W_{3\,\mathrm{exp}}$ should be smaller than zero. Finally, note that both W_3 and $W_{3\,\mathrm{exp}}$ have units of energy per unit area ($\mathrm{J/m^2}$) although it is frequently written as a force per unit length N/m for consistency with the units commonly used to express surface energy γ.

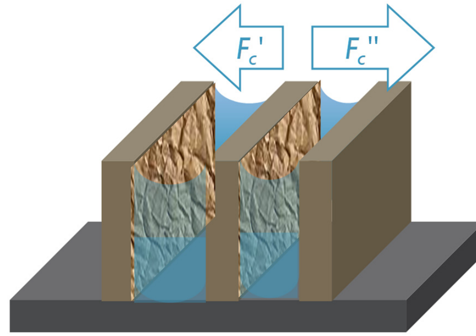

Fig. 1 Unbalanced capillary forces arising at each side of a photoresist line (F'_c and F''_c), owing to sidewall roughness.

2.4 *Unbalanced Capillary Force Acting on Photoresist during Rinse*

Let us consider now the main source of pattern collapse, i.e., the capillary force acting on the sidewalls of photoresist line of height H, trench width S, total surface tension of rinse liquid γ, and contact angle between the photoresist and the rinse liquid, θ

$$F_C = \frac{2\gamma H \cos\theta}{S}. \tag{6}$$

To apply Eq. (6) to our lithography case, consider an ideal dense array of LS consisting of equally spaced lines and trenches of equal width. This situation would bring a perfect equilibrium of capillary forces at each side of each line, and a net zero force acting on the photoresist line. In reality, however, the liquid in the neighbor trenches could have dried unevenly, or the roughness of the line wall is changing the trench width. We discuss how the sidewall roughness, photoresist thickness, and pitch influence the unbalanced capillary force that cause pattern collapse (schematically shown in Fig. 1).

Random fluctuations in the sidewall roughness cause the SWR. SWR can be described as a random variable, normally distributed, of the known mean (equal to the trench CD) and three-sigma standard deviation (measured by CDSEM metrology). The density probability function of the width, X, of the trenches at each side of a given photoresist line is

$$(X = x) = \frac{1}{0.33 \cdot \mathrm{SWR} \cdot \sqrt{2\pi}} e^{-\frac{(x-\mathrm{CD})^2}{2(0.33\cdot\mathrm{SWR})^2}}, \tag{7}$$

where CD is the average trench width and SWR is the three-sigma trench roughness. The net force acting on the unit length of photoresist line (N/m) results from the competition of these two forces

$$F_{\mathrm{line}} = F_C(x') - F_C(x'') = \frac{2\gamma H \cos\theta}{x'} - \frac{2\gamma H \cos\theta}{x''} = 2\gamma H \cos\theta\left(\frac{1}{x'} - \frac{1}{x''}\right), \tag{8}$$

where x' and x'' indicate the trench width at each side of the photoresist line. Interestingly, the cumulative distribution function of F_{line} has no exact solution because the difference of reciprocal normal distributions is not a normal distribution.[25] However, in the Appendix, we show that the probability of F_{line} approximates well a normal distribution with mean equal to zero and standard deviation equal to $\sigma_{F_{\mathrm{line}}} \cong \sqrt{2}\frac{2\gamma h \cos\theta}{\mathrm{CD}^2}\frac{\mathrm{SWR}}{3}$, under certain conditions (SWR < CD) that are also reasonably valid in EUV lithography. In the rest of the paper, the values of F_{line} were calculated numerically in MATLAB.

Finally, we propose a statistical description of the pattern collapse as a probability that the capillary force overcomes the adhesion of unexposed photoresist areas (such as lines, in case of positive-tone processing). The work of adhesion of a line of photoresist length l, width CD, and height h is $W_3 \cdot l \cdot \mathrm{CD}$, and the energy required to peel such a line is $F_{\mathrm{thr}} \cdot l \cdot h$. Neglecting the line length, line collapse happens when the force applied on that line exceeds a threshold force F_{thr}

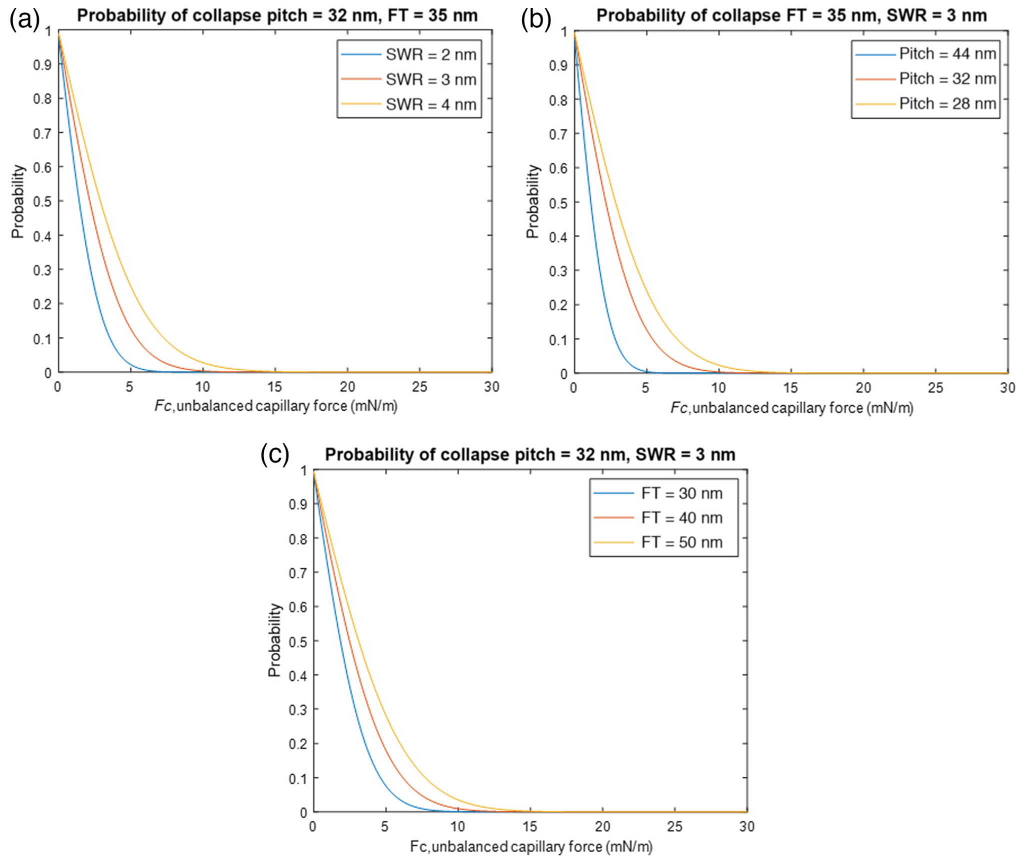

Fig. 2 Threshold force of the unbalance capillary force, calculated by our model: (a) effect of different SWR at pitch 32 nm and film thickness 35 nm; (b) effect of pitch for resist film thickness of 35 nm and SWR 3 nm, and (c) effect of resist film thickness, at pitch 32 nm and SWR = 3 nm. CD of line is always equal to pitch/2.

$$F_{\text{line}} > F_{\text{thr}} = W_3 \cdot \frac{\text{CD}}{h}. \tag{9}$$

The probability of pattern collapse can be estimated using Eqs. (8) and (9) for any line height and width. The simulated results are consistent with experimental observations: the larger the roughness, the smaller the pitch; and the thicker the resist, the more prone is the line to collapse [Figs. 2(a)–2(c), respectively].

3 Results and Discussions

3.1 *Pattern Collapse: W_3 in Unexposed Areas*

Facing the challenge of optimizing the photoresist/underlayer/developer interactions, lithographers are aware that little room is available for changing the surface properties of photoresists. The physicochemical properties of photoresists are already heavily constrained by EUV sensitivity, scanner throughput and productivity, process window, and defectivity. As for the developer liquid, the alkaline developer TMAH has been the undiscussed choice for CAR development for decades and its replacement seems unlikely. As a result, in the following we consider the standpoint of underlayer surface property optimization to maximize EUV lithography process window.

Nine underlayers (A to I) provided by undisclosed materials suppliers were patterned by EUV lithography with the same positive-tone CAR photoresist. For each underlayer, representative images of LS patterns after litho at pitch 32 nm are shown in Fig. 3. In some cases, the

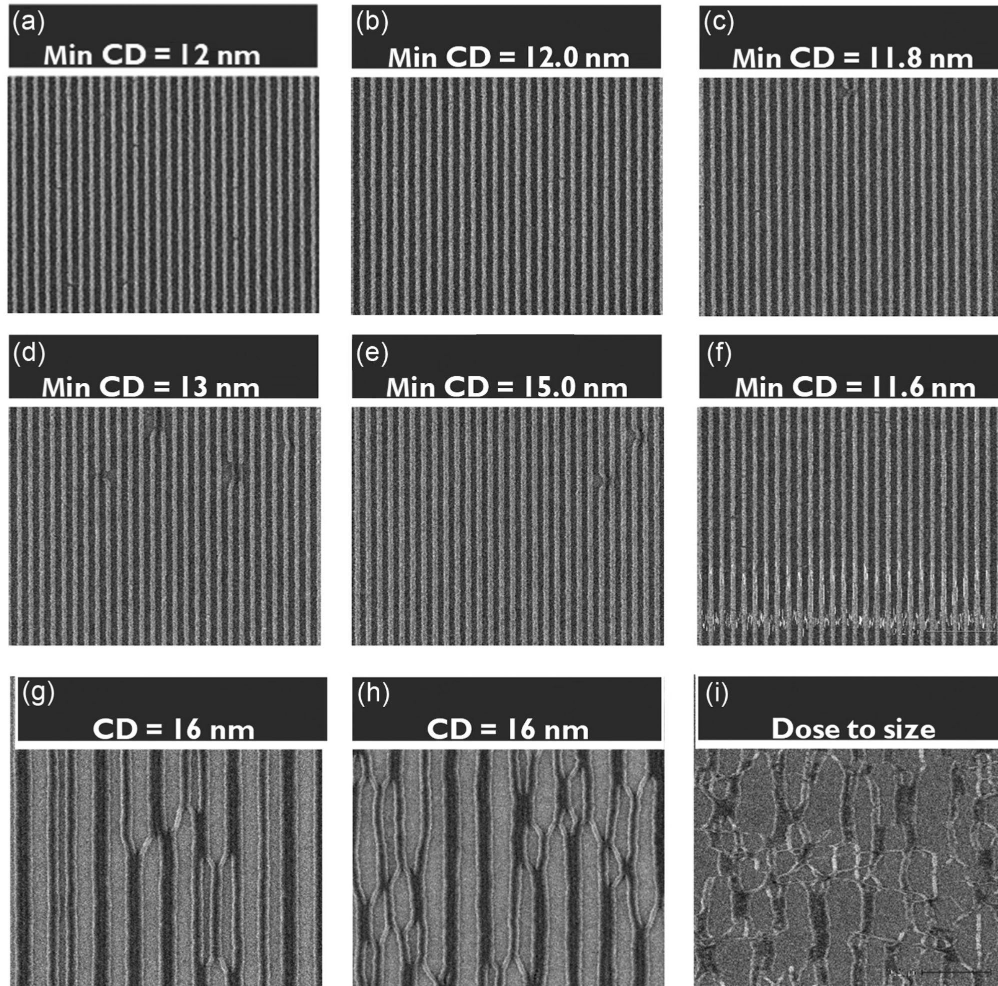

Fig. 3 (a)–(i) Top-down CDSEM images of EUV patterned chemically amplified resist, at pitch 32 nm, on top of nine underlayers. The patterning outcome varies significantly depending on the surface property matching between photoresist and underlayer. Also reported is the smallest line CD at which pattern collapse onsets (Smaller values are better.).

CAR showed catastrophic delamination (H), or patterns collapse and lines merging (G and I) in the entire range of exposure dose and CD. The other samples showed good process window, with varying degrees of collapse margin, with the exception of sample E (very early collapse at CD = 15 nm) and sample F (which showed line breaks before line collapse). For each CDSEM image, the smallest line CD at which the pattern collapse was first observed is reported.

The W_3 factor was calculated for all underlayer surface energy values, based on the surface energy of the specific photoresist and developer used in the experiment. The result is shown in the parameter space $W_3(\gamma^p, \gamma^d)$ of Fig. 4(a), and for the nine underlayers tested (A–I), sorted from highest to smallest, in Fig. 4(b). A good correlation between the W_3 and the collapse probability or margin of Fig. 3 was observed. CAR patterned on underlayers A–C showed a wide process window; underlayers D–F showed early pattern collapse; and samples G–I had unrecoverable delamination at all line CD. Because the CAR photoresist used was the same in all nine samples, the LS height and width were also the same: therefore, the threshold force for pattern collapse only depends on the W_3 factor, which validates our comparison.

3.2 *Photoresist Scumming: $W_{3\,exp}$ in Exposed Areas*

Besides the delamination of the line pattern, our hypothesis was that the adhesion parameter calculated on the exposed areas $W_{3\,\mathrm{exp}}$ would explain and predict photoresist scumming in the

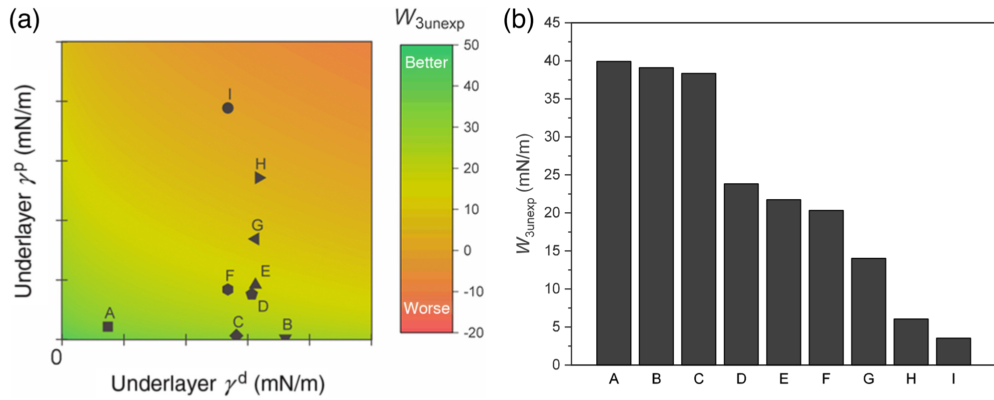

Fig. 4 Calculated W_3 value of unexposed photoresist on nine underlayer samples of (a) varying surface energy components and (b) sorted from highest to lowest. Higher values are better.

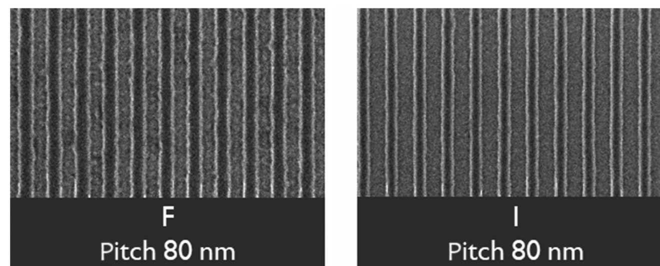

Fig. 5 Top-down CDSEM pictures of pitch 80-nm LS CAR on two selected underlayers, showing clearly different amount of photoresist scumming in the trenches.

trenches between lines. Recognizing photoresist scumming from top-down CDSEM inspection is not straightforward, especially at smaller pitches where the trench CD is ≤20 nm. Scumming can be misjudged with photoresist footing, tapering, or can have other root causes unrelated to photoresist-underlayer-developer interaction. For this reason, we present results on only two of the nine underlayers where the scumming was clearly detectable in relatively widely spaced patterns of pitch 80 nm (i.e., trench width ∼40 nm). The CDSEM pictures of CAR patterned on underlayers *F* and *I* are shown in Fig. 5.

For underlayers *F* and *I*, their location on the $W_{3\ \mathrm{exp}}$ plot was also calculated and shown in Fig. 6. In the case of exposed areas, the calculated value of $W_{3\ \mathrm{exp}}$ is higher for underlayer *F* than it

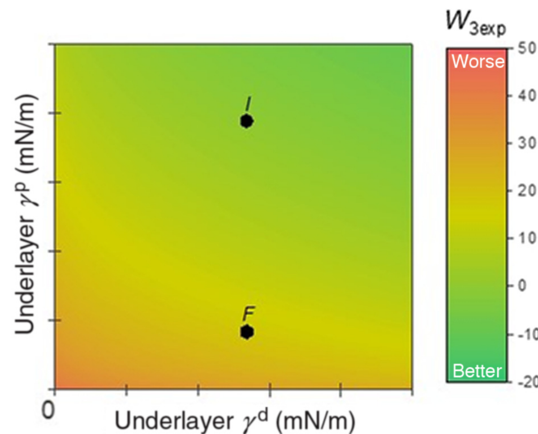

Fig. 6 $W_{3\ \mathrm{exp}}$ factor calculated for the exposed areas (trench, in a positive-tone processing) and location of two underlayers *F* and *I*. Lower values are better.

is for underlayer I, which predicts more photoresist scumming in the former case than in the latter. Our results are in quite good agreement with those reported in previous studies,[7,9] some of which employed a similar approach for EUV photoresists and reached similar results independently.[3,20]

4 Conclusions

We developed a method to estimate adhesion forces in three phases system photoresists-underlayers-developer. A W_3 factor was introduced and experimentally validated to predict pattern collapse and delamination, with a threshold margin determined by the capillary force acting on the photoresist lines. We consider the non-zero net capillary force originating from SWR and describe the probability of pattern collapse at given threshold. Comparison with experimental results shows that our metrics predict both pattern collapse and photoresist scumming satisfactorily. However, our findings also demonstrate that the optima of W_3 and $W_{3\ \mathrm{exp}}$ do not belong to the same range of surface energy. In other words, optimizing simultaneously the patterning in both exposed and unexposed areas can only be achieved as a tradeoff. These metrics are expected to be of interest to materials suppliers who want to optimize the EUV lithography processing, especially when tuning the underlayer physicochemical properties.

5 Appendix: Derivation of the Standard Deviation of the Capillary Force

The probability distribution function of the capillary force acting on a photoresist line given in Eq. (8) as a difference between two reciprocal normal distributions

$$P(F_{\mathrm{line}}) = F_C(x') - F_C(x'') = 2\gamma H \cos\theta\left(\frac{1}{x'} - \frac{1}{x''}\right),$$

where x' and x'' are the random variables representing the width of each trench on either side of the line, normally distributed with the same mean $\bar{x}$, and standard deviation σ_x. Assuming that x' and x'' are uncorrelated, the standard deviation of $P(F_{\mathrm{line}})$ can be propagated[26] approximately as follows:

$$\sigma_{F_\mathrm{approx}} \cong \sqrt{2\left(\frac{\partial P(F)}{\partial x}\right)^2_{x=\bar{x}}\sigma_x^2} = \sqrt{2\left(-\frac{2\gamma h\cos\theta}{\bar{x}^2}\right)^2\sigma_x^2} = \sqrt{2}\frac{2\gamma h\cos\theta}{\bar{x}^2}\sigma_x. \tag{10}$$

In practice, engineers can evaluate the formula by dialing in the trench CD $\bar{x} = CD$ and the three-sigma SWR $\sigma_x = \frac{\mathrm{SWR}}{3}$ obtained from CDSEM metrology. The approximation is valid when $\sigma_x < \bar{x}$. To illustrate this, we calculated the standard deviation of the capillary force using both the approximate formula of Eq. (10) and a numerical solver (MATLAB) for the case of trench $CD = 14$ nm, $p = 28$ nm, line height $h = 30$ nm, angle $\theta = 77.5$ deg, three-sigma SWR $=$ 3 nm. The resulting $\sigma_{F_\mathrm{approx}} = 3.9729$ mN/m was within $\pm 1\%$ of the numerical value $\sigma_{F_{\mathrm{MATLAB}}} = 4.0114$ mN/m. All values used are typical for EUV lithography and validate the usage of Eq. (8) for all practical purposes.

Acknowledgments

The authors wish to thank Nadia Vandenbroeck (IMEC) and Saika M. Bari (Karlsruhe Institute of Technology) for technical support and Pieter Vanelderen (IMEC) for initial experiments on the topic. The authors declare no conflict of interest.

References

1. J. van Schoot et al., "High-NA EUV lithography exposure tool: advantages and program progress," *Proc. SPIE* **11517**, 1151712 (2020).
2. P. Vanelderen et al., "Underlayer optimization method for EUV lithography," *Proc. SPIE* **11326**, 1132615 (2020).

3. H. Yaegashi et al., "Explorations of missing hole defect in EUV patterning," *Proc. SPIE* **11326**, 113260E (2020).
4. D. L. Goldfarb et al., "Pattern collapse mitigation strategies for EUV lithography," *Proc. SPIE* **8322**, 832205 (2012).
5. D. L. Goldfarb et al. "Fundamentals of EUV resist-inorganic hardmask interactions," *Proc. SPIE* **10146**, 101467 (2017).
6. K. Petrillo et al., "Line width roughness control and pattern collapse solutions for EUV patterning," *Proc. SPIE* **7969**, 796913 (2011).
7. K. Takahashi and A. Kawai, "Effect of low surface tension developer on micro bubble removal from resist square window pattern," *J. Phot. Sci. Technol.* **26**, 765 (2013).
8. R. Gronheid, "Impact of development chemistry on extreme ultraviolet resist performance," *J. Vac. Sci. Technol. B.* **28**, C6S1 (2010).
9. M. Harumoto et al., "Alternative developer solutions and processes for EUV and ArFi lithography," *J. Phot. Sci. Technol.* **32**(2), 321 (2019).
10. M. Padmanaban et al., "Underlayer and rinse materials for improving EUV resist performance," *Proc. SPIE* **8682**, 868215 (2013).
11. D. H. Kaelble, "Dispersion-polar surface tension properties of organic solids," *J. Adhesion* **2**, 66 (1970).
12. D. K. Owens and R. C. Wendt, "Estimation of the surface free energy of polymers," *J. Appl. Polym. Sci.* **13**, 1741 (1969).
13. B. Song, "Determination of interfacial tension from the profile of a pendant drop using computer-aided image processing: 2. Experimental," *J. Colloid Interface Sci.* **184**(1), 77 (1996).
14. M. Kramkowska and I. Zubel, "Silicon anisotropic etching in KOH and TMAH with modified surface tension," *Procedia Chem.* **1**, 774 (2009).
15. F. M. Fowkes, "Attractive forces at interfaces," *Ind. Eng. Chem.* **56**, 40 (1964).
16. K. L. Johnson et al., "Surface energy and contact of elastic solids," *Proc. R. Soc. Lond.* **324**(1558), 301 (1971).
17. S. Wu, "Calculation of interfacial tension in polymer systems," *J. Polym. Sci. C* **34**, 19 (1971).
18. F. L. Leite et al., "Theoretical models for surface forces and adhesion and their measurement using atomic force microscopy," *Int. J. Mol. Sci.* **13**, 12773 (2012).
19. J. H. Sim et al., "Thickness dependence of properties of EUV underlayer thin films," *Proc. SPIE* **12055**, 120550B (2022).
20. S. Okada et al., "Enabling EUV pattern transfer by optimized under layer," *Proc. SPIE* **11612**, 116120V (2021).
21. J. Comyn, *Adhesive Bonding*, R. D. Adams, 2nd ed., p. 41 (2021).
22. S. Ozbay et al., "Surface free energy and wettability properties of transparent conducting oxide-based films with Ag interlayer," *Appl. Surf. Sci.* **567**, 150901 (2021).
23. T. Funasaka et al., "Adhesive ability and solvent solubility of propylene-butene copolymers modified with maleic anhydride," *Int. J. Adhesion Adhes.* **19**, 367 (1999).
24. R. S. Wise, "Breaking stochastic tradeoffs with a dry deposited and dry developed EUV photoresist system," *Proc. SPIE* **11612**, 1161203 (2021).
25. C. Lecomte, "Exact statistics of systems with uncertainties: An analytical theory of rank-one stochastic dynamic systems," *J. Sound Vibr.* **332**(11), 2750 (2013).
26. J. R. Taylor, *An Introduction to Error Analysis: The Study of Uncertainties in Physical Measurements*, 2nd ed., University Science Books (1997).

Roberto Fallica is a staff researcher at the Interuniversitair Microelectronica Centrum (IMEC) in Leuven, Belgium. He received his E Eng. degree from Politecnico di Milano, Italy, and his PhD from the University of Milano-Bicocca, Italy. He was a post-doc researcher at the Paul Scherrer Institute where he worked on X-ray interference lithography doing characterization of photo-sensitive materials for patterning with extreme ultraviolet light. He is the author of more than 50 journal papers and proceedings and has written one book chapter. He is a member of SPIE.

Biographies of the other authors are not available.